Scientific Research Publishing

Advances in Materials Physics and Chemistry, 2022, 12, 47-57
https://www.scirp.org/journal/ampc
ISSN Online: 2162-5328
ISSN Print: 2162-531X

Influence of Deposition Temperature on the Electrical and Electrochemical Properties of Carbon-Based Coatings for Metallic Bipolar Plates, Prepared by Cathodic Arc Evaporation

Maximilian Steinhorst[1,2*], Maurizio Giorgio[1], Teja Roch[1], Christoph Leyens[1,2]

[1]Fraunhofer Institute for Material and Beam Technology IWS, Dresden, Germany
[2]Institute of Material Science, Technische Universität Dresden, Dresden, Germany
Email: *maximilian.steinhorst@iws.fraunhofer.de

How to cite this paper: Steinhorst, M., Giorgio, M., Roch, T. and Leyens, C. (2022) Influence of Deposition Temperature on the Electrical and Electrochemical Properties of Carbon-Based Coatings for Metallic Bipolar Plates, Prepared by Cathodic Arc Evaporation. *Advances in Materials Physics and Chemistry*, **12**, 47-57.
https://doi.org/10.4236/ampc.2022.124004

Received: December 29, 2021
Accepted: April 17, 2022
Published: April 20, 2022

Abstract

Cathodic arc evaporation is a well-established physical vapor deposition technique which is characterized by a high degree of ionization and high deposition rate. So far, this technique has been mainly used for the deposition of tribological coatings. In this study, anti-corrosive and electrical conductive carbon-based coatings with a metallic interlayer were prepared on stainless steel substrates as surface modification for metallic bipolar plates. Hereby, the influence of the deposition temperature during the deposition of the carbon top layer was investigated. Raman spectroscopy revealed differences in the microstructure at 200˚C compared to 300˚C and 100˚C. Measurements of the interfacial contact resistance showed that the deposited coatings significantly improve the electrical conductivity. There are only minor differences between the different carbon top layers. The corrosion resistance of the coatings was studied via potentiodynamic polarization at room temperature and 80˚C. Experiments showed that the coating with a carbon top layer deposited at 200˚C, considerably reduces the current density and thus corrosion of the substrate is suppressed.

Keywords

Bipolar Plate, Corrosion, Interfacial Contact Resistance, Carbon Thin Film, Physical Vapor Deposition

1. Introduction

In consideration of the high energy demand, the development of efficient and

eco-friendly energy systems is crucial [1]. Polymer electrolyte membrane fuel cells (PEMFC) exhibit good efficiency and high user convenience, including long travel distances and fast refuelling cycles, rendering them as a key technology towards climate-friendly mobility [2] [3]. The bipolar plate (BPP) is an important component of a PEMFC since it is responsible for the distribution of hydrogen and oxygen, cooling and electrical connection. Thus, it must fulfill a variety of requirements such as good mechanical stability, high corrosion resistance and good electrical as well as thermal conductivity. Austenitic stainless steel is a potential material candidate to replace the graphite and composite bipolar plates. Especially, 316L stainless steel exhibits a promising combination of properties [4] [5] [6] [7]. However, the native oxide reduces the electrical contact to the adjacent gas-diffusion layer (GDL) and the steel corrodes in the harsh PEMFC operating conditions [8] [9]. The interfacial contact resistance (ICR) between the BPP and GDL can significantly affect the efficiency of a fuel cell stack, because it contributes to a great extent to the ohmic resistance in a fuel cell [10] [11] [12]. Due to the corrosion, harmful metal ions can be released and contaminate the membrane reducing the longevity of PEMFCs [13] [14].

In order to prevent corrosion and simultaneously increase the electrical conductivity, a variety of BPP surface modifications were studied such as pure metallic and various metallic compounds [8] [15]-[20] as well as different carbon-based thin films [21]-[28] as either single or multi layer coatings. Hereby, carbon-based coatings exhibit excellent properties such as high chemical inertness and low electrical resistance [29]. However, the thin films are usually produced by balanced or unbalanced magnetron sputtering and (plasma-enhanced) chemical vapor deposition which have a low ionization and deposition rate. In this context, cathodic arc evaporation which is a well-established physical vapor deposition (PVD) method for tribological carbon coatings, has favorable properties, e.g. generation of a highly ionized plasma and fast deposition rate [30] [31]. Additionally, the deposition temperature is an important parameter which can significantly affect the properties of a PVD coating [32].

In this study, we investigate the electrical and electrochemical properties of carbon-based coatings on 316L stainless steel (SS316L) substrates depending on the deposition temperature. Three different carbon thin films were prepared by varying the temperature during the deposition. All samples have the same metallic interlayer.

2. Experimental

2.1. Materials

Austenitic stainless steel (SS316L) of 0.1 mm thickness was used as substrate material. The specimens were cleaned with distilled water, methanol and then dried with nitrogen prior to deposition. For the deposition of the carbon-based coatings, a cathodic arc deposition system was used. The base pressure of the

vacuum chamber was set at 10^{-4} Pa. Before coating, the native oxide layer of the steel substrates was removed by a plasma etching process. A chromium interlayer was deposited on the cleaned substrates, from a pure chromium target (99.99%), at a chamber temperature of 300˚C and pressure of approximately 10^{-1} Pa. Afterwards, three different carbon top layer variants were deposited from a 99.99% graphite target in the deposition temperature range between 300˚C and 100˚C. Bias voltage of several hundred of volts and pressure of approximately 10^{-1} Pa were kept constant for all carbon thin films. The total thickness, measured by X-ray reflectivity, of the deposited thin films was approximately 60 - 66 nm.

2.2. Characterization Methods

Raman spectroscopy was used to evaluate the microstructure of the deposited thin films. The measurements were done with a Renishaw inVia and an excitation laser of 514 nm wavelength. For the evaluation of the D peak and G peak, a Lorentzian and a Breit-Wigner-Fano function were used, respectively.

The interfacial contact resistance was determined similar to the procedure described from Davies *et al.* [4] and Wang *et al.* [5]. In brief, the measurement setup consits of a tensile tester for applying the compaction force and an electrical circuit attached to two gold-coated copper blocks with two GDL sheets and a sample in-between. The total resistance of the assembly is measured by an ohmmeter. By measuring the contact resistance of one GDL sample, which is also used for calibration, one can calculate the individual contact resistance of the sample. For the measurements the compaction force ranged from 25 to 200 $N \cdot cm^{-2}$.

Corrosion resistance was investigated by potentiodynamic polarization tests in 0.5 M H_2SO_4 solution at room temperature and 80˚C. For this purpose, a Metrohm Autolab PGSTAT302N potentio-/galvanostat was used with a three-electrode setup including a graphite rod as counter electrode, a Ag/AgCl reference and the sample as working electrode. Before the potentiodynamic tests, the open circuit potential was recorded for a duration of 1 h. The measurements were performed between −0.5 to 1.5 V vs. standard hydrogen electrode (SHE) at a scan rate of 0.001 $V \cdot s^{-1}$.

3. Results and Discussion

3.1. Material characterization

Raman spectra of carbon films are mainly composed of two broad peaks at around 1350 cm^{-1} and 1580 - 1600 cm^{-1}, namely D and G peak, respectively. The G peak (graphite) is related to the graphite lattice and the bond stretching of all sp^2 atoms, and the D peak (defect) results from the breathing modes of carbon rings and defects in the graphite crystalline structure [33]. **Figure 1** shows the recorded Raman spectra of the deposited thin films. Whilst, the films deposited at 300˚C and 100˚C exhibit similar spectra and have pronounced D and G peaks (see **Figure 1(a)**), the 200˚C carbon thin film only has small peaks (see **Figure 1(b)**).

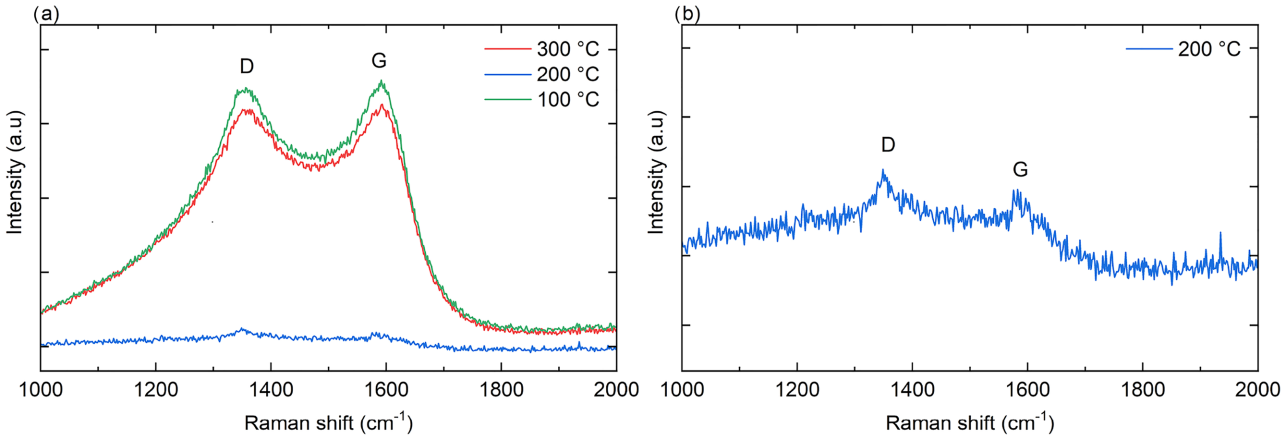

Figure 1. (a) Raman spectra of the coated samples with a carbon top layer deposited at 300˚C, 200˚C and 100˚C. (b) Enlarged Raman spectrum of the coated sample with a carbon top layer deposited at 200˚C.

The shape of this Raman spectrum corresponds to a more disordered structure as described by Onoprienko *et al.* [34] and Chung *et al.* [35].

The full width half maximum (FWHM) and position of the G peak are associated with disorder in the film structure, *i.e.* distortion of bond length and angle in six-fold carbon rings which originates from poor graphitic in-plane ordering [36] [37]. Additionally, higher I_D/I_G and G peak position indicates a higher sp^2 content in the material. According to **Table 1**, the carbon top layers deposited at 300˚C and 100˚C are likely to exhibit a similar microstructure. In comparison to that, the 200˚C carbon thin film has a significantly higher intensity ratio I_D/I_G of 1.59 and G peak position. Moreover, the FWHM of the G peak is the lowest of the samples and together with the other Raman parameters this indicates that the carbon top layer deposited at 200˚C might have a different microstructure but still a very high sp^2 content. This is in good agreement with the evaluation of carbon Raman spectra from Ferrari *et al.* [33] [36] [38].

J. Robertson [30] reported that for G peak FWHM values above 50 cm^{-1} the graphite crystallites are less than or equal to 2 nm in size. In this region it is possible to determine the grain size L_a by

$$I_D/I_G = cL_a^2 \tag{1}$$

where L_a is in Å and c is a constant approximately equal to 0.0055 [36]. Thus, the carbon thin films in this work have a grain size of 1.34 nm, 1.70 nm and 1.32 nm, respectively. Based on the results, the deposited carbon top layers can be classified as graphite-like carbon or nano-crystalline carbon with probably up to 100% sp^2 content.

3.2. Interfacial Contact Resistance

The interfacial contact resistance between the metallic BPP and the GDL has a significant impact on the achieved electrical power (output) of a PEMFC. Hence, a low ICR is necessary for bipolar plates and corresponding surface modifications. **Figure 2** shows the ICR as a function of the applied compaction force for

Table 1. Raman parameters of the coated samples with a carbon top layer deposited at 300˚C, 200˚C and 100˚C.

Carbon deposition temperature	I_D/I_G	G peak position (cm^{-1})	FWHM G (cm^{-1})	FWHM D (cm^{-1})
300˚C	0.99	1593	141	277
200˚C	1.59	1601	107	353
100˚C	0.96	1594	128	200

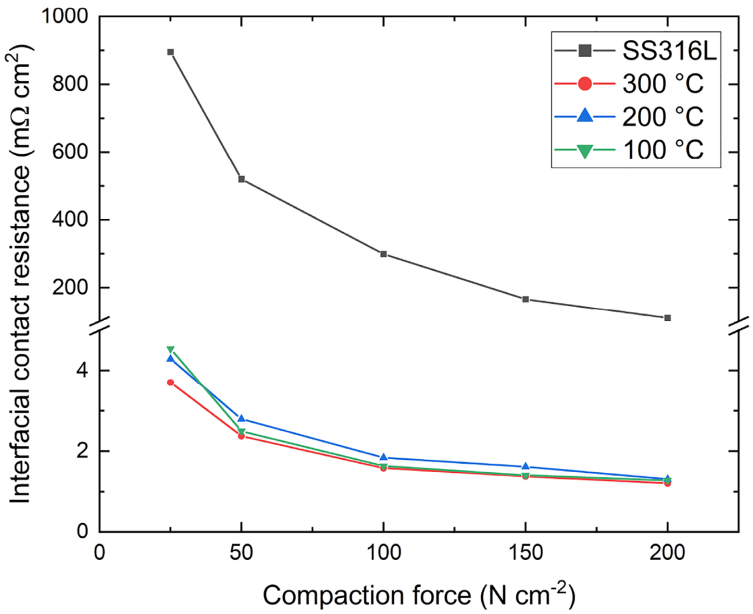

Figure 2. Interfacial contact resistance as a function of applied compaction force of the bare SS316 substrate and the coated samples with a carbon top layer deposited at 300˚C, 200˚C and 100˚C.

the carbon-based coatings depending on the carbon deposition temperature. Up to a compaction of 100 N/cm², the contact resistance rapidly decreases because of the constant increase in the contact area between the GDL and the specimen. The bare SS316L substrate exhibits the highest ICR values which can be attributed to the native oxide layer. This underlines the need for highly conductive coatings. By applying a carbon-based coating, the ICR is reduced by more than two orders of magnitude. There are only small differences between the carbon layers deposited at different temperatures. However, the sample with a carbon top layer deposited at 200˚C has the highest resistance in the measurement range. Still, all carbon-based coatings more than fulfill the criteria, released by the U.S. department of energy, of 10 mΩ·cm² [39] and achieve values less than 2 mΩ·cm² at 150 N/cm².

3.3. Potentiodynamic Polarization

The potentiodynamic polarization curves of all specimens at room temperature in 0.5 M H_2SO_4 are depicted in **Figure 3**. The bare SS316L substrate has the lowest

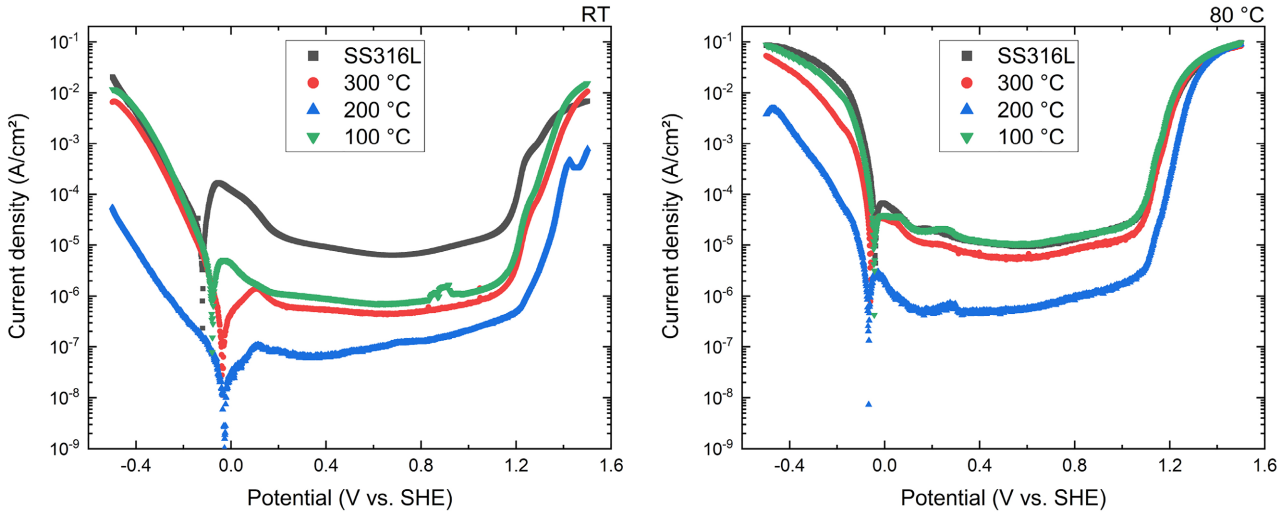

Figure 3. Potentiodynamic polarization curves of the bare SS316 substrate and the coated samples with a carbon top layer deposited at 300˚C, 200˚C and 100˚C. The tests were conducted in 0.5 M H_2SO_4 at room temperature (left) and 80˚C (right) bubbled with argon.

Table 2. Corrosion parameters of bare SS316L and the coated samples with a carbon top layer deposited at 300˚C, 200˚C and 100˚C. The experimental conditions were 0.5 M H_2SO_4 at room temperature and 80˚C bubbled with argon.

Sample	RT		80˚C	
	E_{corr} (V)	j_{corr} (A·cm^{-2})	E_{corr} (V)	j_{corr} (A·cm^{-2})
SS316L	−0.118	1.76×10^{-5}	−0.039	1.55×10^{-4}
300˚C	−0.037	2.58×10^{-7}	−0.060	3.33×10^{-5}
200˚C	−0.028	3.46×10^{-9}	−0.067	3.34×10^{-5}
100˚C	−0.079	4.84×10^{-6}	−0.044	5.98×10^{-5}

corrosion resistance and thus the highest corrosion current j_{corr} of approx. 1.8×10^{-5} A·cm^{-2} (see Table 2). At around 0 V the formation of a protective oxide layer begins, which can be seen by the strong oxidation peak. Up to a potential of 1.2 V, the stainless steel remains inert in the environment and above this potential the material enters the transpassive state. Here, the dissociation of the electrolyte (*i.e.* water) occurs as well. This results in a steep increase in the current signal which can also be observed for the coated samples.

The deposition of a carbon-based coating greatly improves the corrosion resistance leading to a significantly lower corrosion current j_{corr} between 10^{-6} and 10^{-9} A·m^{-2} (see Table 2). Structural properties such as surface morphology, grain size and defects affect the corrosion resistance of a material and thus the corrosion current density [40]. Consequently, the microstructure of a surface modification, *i.e.* a PVD coating, is an important parameter. The considerable lower current density of the 200˚C carbon top layer can be attributed to its different microstructure compared to the other carbon thin films.

At an electrolyte temperature of 80˚C, the differences between the polariza-

tion curves are less distinct except for the sample with a carbon top layer deposited at 200˚C (see Figure 3, right). In general, the increased temperature leads to a more aggressive environment and hence more corrosion. This can be seen by the clear shift towards higher current densities and thus significantly higher corrosion currents j_{corr} (see Table 2). In the case of the 100˚C carbon top layer, the rise in j_{corr} is particularly pronounced. In contrast, the 200˚C carbon top layer still has a very low corrosion current. Again, this is likely due to structural differences (see Figure 1) and thus better corrosion protection of the SS316L substrate.

4. Conclusions

Three multi layer coatings consisting of a metallic interlayer and a carbon top layer deposited at different temperatures were prepared in order to investigate the influence of the deposition temperature on the electrical and electrochemical properties. The coatings were analyzed by Raman spectroscopy, interfacial contact resistance measurements and potentiodynamic polarization tests in 0.5 M H_2SO_4.

The material analysis revealed that the carbon top layers deposited at 300˚C and 100˚C likely have a similar microstructure because of comparable Raman parameters such as intensity ratio I_D/I_G and G peak position. Due to the significantly higher I_D/I_G of 1.59 and low FWHM G of 107, it is likely that the 200˚C carbon thin film exhibits differences in the microstructure. The shift of G peak position to approximately 1600 cm^{-1} and larger crystallite size L_a of 1.7 nm, compared to 1594 cm^{-1} and 1.3 nm, respectively, indicate a structural change.

The uncoated substrate exhibits the highest interfacial contact resistance of all samples due to the native oxide layer. By applying a carbon-based coating, the resistance is significantly reduced. There are only minor differences between the different carbon top layers. However, the carbon thin film deposited at 200˚C exhibits the highest resistance values among the coated samples. Still, all have an ICR lower than 2 $m\Omega \cdot cm^2$ at 150 $N \cdot cm^{-2}$, which is well below the DOE criteria of 10 $m\Omega \cdot cm^2$.

A significant improvement of corrosion resistance due to the application of a carbon-based coating can be observed in the polarization curves. Here, the 200˚C carbon top layer exhibits the lowest corrosion current of below 10^{-8} A cm^{-2}. In this context, the two other coatings with similar Raman parameters have comparable electrochemical properties. At an elevated electrolyte temperature of 80˚C, the corrosive attack is increased and thus higher current densities can be observed for all samples. However, the carbon top layer deposited at 200˚C exhibits still the best corrosion protection.

In general, the results show that carbon-based coatings offer a good corrosion protection with excellent electrical conductivity at the same time. It is possible to prepare these coatings at low deposition temperatures of 200˚C or even 100˚C, which is of great advantage for a future production of coated bipolar plates.

However, further investigations regarding the electrochemical properties are required to increase the service life of a fuel cell. In this context, the microstructure of the carbon thin films will be further examined and the development of alternative interlayer materials will be considered in future studies.

Acknowledgements

The authors would like to acknowledge the financial support from the Fraunhofer internal research project HOKOME.

Conflicts of Interest

The authors declare no conflicts of interest regarding the publication of this paper.

References

[1] International Energy Agency (2020) Global Energy Review 2019. Technical Report, International Energy Agency, Paris. https://www.iea.org/reports/global-energy-review-2019

[2] Carrette, L., Friedrich, K. and Stimming, U. (2000) Fuel Cells: Principles, Types, Fuels, and Applications. *ChemPhysChem*, **1**, 162-193. https://doi.org/10.1002/1439-7641(20001215)1:4%3C162::AID-CPHC162%3E3.0.CO;2-Z

[3] Gröger, O., Gasteiger, H. and Suchsland, J. (2015) Review-Electromobility: Batteries or Fuel Cells? *Journal of the Electrochemical Society*, **162**, A2605-A2622. https://doi.org/10.1149/2.0211514jes

[4] Davies, D., Adcock, P., Turpin, M. and Rowen, S. (2000) Stainless Steel as a Bipolar Plate Material for Solid Polymer Fuel Cells. *Journal of Power Sources*, **86**, 237-242. https://doi.org/10.1016/S0378-7753(99)00524-8

[5] Wang, H., Sweikart, M. and Turner, J. (2003) Stainless Steel as Bipolar Plate Material for Polymer Electrolyte Membrane Fuel Cells. *Journal of Power Sources*, **115**, 243-251. https://doi.org/10.1016/S0378-7753(03)00023-5

[6] Tawfik, H., Hung, Y. and Mahajan, D. (2007) Metal Bipolar Plates for PEM Fuel Cell—A Review. *Journal of Power Sources*, **163**, 755-767. https://doi.org/10.1016/j.jpowsour.2006.09.088

[7] Xu, Z., Qiu, D., Yi, P., Peng, L. and Lai, X. (2020) Towards Mass Applications: A Review on the Challenges and Developments in Metallic Bipolar Plates for PEMFC. *Progress in Natural Science*: *Materials International*, **30**, 815-824. https://doi.org/10.1016/j.pnsc.2020.10.015

[8] Yoon, W., Huang, X., Fazzino, P., Reifsnider, K. and Akkaoui, M. (2008) Evaluation of Coated Metallic Bipolar Plates for Polymer Electrolyte Membrane Fuel Cells. *International Journal of Electrochemical Science*, **179**, 265-273. https://doi.org/10.1016/j.jpowsour.2007.12.034

[9] Asri, N., Husaini, T., Sulong, A., Majlan, E. and Daud, W. (2017) Coating of Stainless Steel and Titanium Bipolar Plates for Anticorrosion in PEMFC: A Review. *International Journal of Hydrogen Energy*, **42**, 9135-9148. https://doi.org/10.1016/j.ijhydene.2016.06.241

[10] Makkus, R.C., Janssen, A.H., De Bruijn, F.A. and Mallant, R.K.A.M. (2000) Use of

Stainless Steel for Cost Competitive Bipolar Plates in the SPFC. *Journal of Power Sources*, **86**, 274-282. https://doi.org/10.1016/S0378-7753(99)00460-7

[11] Mohr, P. (2018) Optimierung Von Brennstoffzellen-Bipolarplatten Für Die Automobile Anwendung. Ph.D. Dissertation, University Duisburg-Essen, Duisburg. https://duepublico2.uni-due.de/receive/duepublico_mods_00045782

[12] Liang, P., Qiu, D., Peng, L., Yi, P., Lai, X. and Ni, J. (2018) Contact Resistance Prediction of Proton Exchange Membrane Fuel Cell Considering Fabrication Characteristics of Metallic Bipolar Plates. *Energy Conversion and Management*, **169**, 334-344. https://doi.org/10.1016/j.enconman.2018.05.069

[13] Pozio, A., Silva, R., Francesco, M.D. and Giorgi, L. (2003) Nafion Degradation in PEFCS from End Plate Iron Contamination. *Electrochimica Acta*, **48**, 1543-1549. https://doi.org/10.1016/S0013-4686(03)00026-4

[14] Cheng, X., Shi, Z., Glass, N., Zhang, L., Zhang, J., Song, D., Liu, Z.-S., Wang, H. and Shen, J. (2007) A Review of PEM Hydrogen Fuel Cell Contamination: Impacts, Mechanisms, and Mitigation. *Journal of Power Sources*, **165**, 739-756. https://doi.org/10.1016/j.jpowsour.2006.12.012

[15] Kim, J.-H., Kim, S.-K.., You, Y.-Z., Kim, D.-I., Hong, S.-T., Suh, H.-C. and Weil, K. (2011) Niobium Sputter Coated Stainless Steel as a Bipolar Plate Material for Polymer Electrolyte Membrane Fuel Cell Stacks. *International Journal of Electrochemical Science*, **6**, 4365-4377.

[16] Zhang, H., Lin, G., Hou, M., Hu, L., Han, Z., Fu, Y., Shao, Z. and Yi, B. (2012) CrN/Cr Multilayer Coating on 316l Stainless Steel as Bipolar Plates for Proton Exchange Membrane Fuel Cells. *Journal of Power Sources*, **198**, 176-181. https://doi.org/10.1016/j.jpowsour.2011.09.091

[17] Huang, N., Yu, H., Xu, L., Zhan, S., Sun, M. and Kirk, D. (2016) Corrosion Kinetics of 316l Stainless Steel Bipolar Plate With Chromiumcarbide Coating in Simulated PEMFC Cathodic Environment. *Results in Physics*, **6**, 730-736. https://doi.org/10.1016/j.rinp.2016.10.002

[18] Wang, S., Hou, M., Zhao, Q., Jiang, Y., Wang, Z., Li, H., Fu, Y. and Shao, Z. (2019) Ti/(Ti,Cr)N/CrN Multilayer Coated 316l Stainless Steel by Arc Ion Plating as Bipolar Plates for Proton Exchange Membrane Fuel Cells. *Journal of Energy Chemistry*, **26**, 168-174. https://doi.org/10.1016/j.jechem.2016.09.004

[19] Manso, A., Marzo, F., Garicano, X., Alegre, C., Lozano, A. and Barreras, F. (2020) Corrosion Behavior of Tantalum Coatings on AISI 316l Stainless Steel Substrate for Bipolar Plates of PEM Fuel Cells. *International Journal of Hydrogen Energy*, **45**, 20679-20691. https://doi.org/10.1016/j.ijhydene.2019.12.157

[20] Xu, M., Kang, S., Lu, J., Yan, X., Chen, T. and Wang, Z. (2020) Properties of a Plasma-nitrided Coating and a CrNx Coating on the Stainless Steel Bipolar Plate of PEMFC. *Coatings*, **10**, Article No. 183. https://doi.org/10.3390/coatings10020183

[21] Yi, P., Peng, L., Feng, L., Gan, P. and Lai, X. (2010) Performance of a Proton Exchange Membrane Fuel Cell Stack Using Conductive Amorphous Carbon-Coated 304 Stainless Steel Bipolar Plates. *Journal of Power Sources*, **195**, 7061-7066. https://doi.org/10.1016/j.jallcom.2011.04.044

[22] Larijani, M., Yari, M., Afshar, A., Jafarian, M. and Eshghabadi, M. (2011) A Comparison of Carbon Coated and Uncoated 316l Stainless Steel for Using as Bipolar Plates in PEMFCs. *Journal of Alloys and Compounds*, **509**, 7400-7404. https://doi.org/10.1016/j.jallcom.2011.04.044

[23] Husby, H., Kongstein, O., Oedegaard, A. and Seland, F. (2014) Carbonpolymer Composite Coatings for PEM Fuel Cell Bipolar Plates. *International Journal of Hy-*

drogen Energy, **39**, 951-957. https://doi.org/10.1016/j.ijhydene.2013.10.115

[24] Mingge, W., Congda, L., Tao, H., Guohai, C., Donghui, W., Haifeng, Z., Dong, Z. and Aiying, W. (2016) Chromium Interlayer Amorphous Carbon Film for 304 Stainless Steel Bipolar Plate of Proton Exchange Membrane Fuel Cell. *Surface and Coatings Technology*, **307**, 374-381. https://doi.org/10.1016/j.surfcoat.2016.07.069

[25] Mingge, W., Congda, L., Guohai, T.D.A.C., Donghui, W., Haifeng, Z., Dong, Z. and Aiying, W. (2016) Effects of Metal Buffer Layer for Amorphous Carbon Film of 304 Stainless Steel Bipolar Plate. *Thin Solid Films*, **616**, 507-514. https://doi.org/10.1016/j.tsf.2016.07.043

[26] Steinhorst, M., Giorgio, M., Topalski, S. and Roch, T. (2019) Investigation of Carbon-Based Coatings on Austenitic Stainless Steel for Bipolar Plates in Proton Exchange Membrane Fuel Cells, Produced by Cathodic Arc Deposition. *Proceedings of the FC³—1st Fuel Cell Conference Chemnitz* 2019-*Saubere Antriebe*, *Effizient Produziert*, Chemnitz, 26-27 November 2019, 1-8. https://nbn-resolving.org/urn:nbn:de:bsz:ch1-qucosa2-361973

[27] Hu, R., Tang, J., Zhu, G., Deng, Q. and Lu, J. (2019) the Effect of Duty Cycle and Bias Voltage for Graphite-Like Carbon Film Coated 304 Stainless Steel as Metallic Bipolar Plate. *Journal of Alloys and Compounds*, **772**, 1067-1078. https://doi.org/10.1016/j.jallcom.2018.09.169

[28] Alaefour, I., Shahgaldi, S., Zhao, J. and Li, X. (2021) Synthesis and Ex-situ Characterizations of Diamond-Like Carbon Coatings for Metallic Bipolar Plates in PEM Fuel Cells. *International Journal of Hydrogen Energy*, **46**, 11059-11070. https://doi.org/10.1016/j.ijhydene.2020.09.259

[29] Yi, P., Zhang, D., Qiu, D., Peng, L. and Lai, X. (2019) Carbon-Based Coatings for Metallic Bipolar Plates Used in Proton Exchange Membrane Fuel Cells. *International Journal of Hydrogen Energy*, **44**, 6813-6843. https://doi.org/10.1016/j.ijhydene.2019.01.176

[30] Robertson, J. (2002) Diamond-Like Amorphous Carbon. *Materials Science and Engineering*: *R*: *Reports*, **37**, 129-281. https://doi.org/10.1016/S0927-796X(02)00005-0

[31] Schultrich, B. (2018) Tetrahedrally Bonded Amorphous Carbon Films I. 1st Edition, Springer, Berlin, Heidelberg. https://doi.org/10.1007/978-3-662-55927-7

[32] Mattox, D. (2010) Handbook of Physical Vapor Deposition (PVD) Processing. 2nd Edition, William Andrew, Norwich. https://doi.org/10.1016/C2009-0-18800-1

[33] Ferrari, A. and Robertson, J. (2004) Raman Spectroscopy of Amorphous, Nanostructured, Diamond-Like Carbon, and Nanodiamond. *Philosophical Transactions of the Royal Society of London*. *Series A*: *Mathematical*, *Physical and Engineering Sciences*, **362**, 2477-2512. https://doi.org/10.1098/rsta.2004.1452

[34] Onoprienko, A.A., Artamonov, V.V. and Yanchuk, I.B. (2003) Effect of Deposition and Anneal Temperature on the Resistivity of Magnetron Sputtered Carbon Films. *Surface and Coatings Technology*, **172**, 189-193. https://doi.org/10.1016/S0257-8972(03)00333-5

[35] Chung, C.-Y., Chen, S.-K., Chiu, P.-J., Chang, M.-H., Hung, T.-T. and Ko, T.-H. (2008) Carbon Film-Coated 304 Stainless Steel as Pemfc Bipolar Plate. *Journal of Power Sources*, **176**, 276-281. https://doi.org/10.1016/j.jpowsour.2007.10.022

[36] Ferrari, A. and Robertson, J. (2000) Interpretation of Raman Spectra of Disordered and Amorphous Carbon. *Physical Review B*, **61**, 14095-14107. https://doi.org/10.1103/PhysRevB.61.14095

[37] Baptista, D. and Zawislak, F. (2004) Hard and Sp^2-Rich Amorphous Carbon Structure Formed by Ion Beam Irradiation of Fullerene, *a*-C and Polymeric *a*-C:H Films.

Diamond and Related Materials, **13**, 1791-1801.
https://doi.org/10.1016/j.diamond.2004.04.006

[38] Ferrari, A. and Robertson, J. (2001) Resonant Raman Spectroscopy of Disordered, Amorphous, and Diamondlike Carbon. *Physical Review B*, **362**, Article ID: 075414.
https://doi.org/10.1103/PhysRevB.64.075414

[39] Hydrogen and Fuel Cell Technologies Office (2017) Hydrogen and Fuel Cell Technologies Office Multi-Year Research, Development, and Demonstration Plan. Technical Report, U.S. Department of Energy, Washington DC.
https://www.energy.gov/sites/default/files/2017/05/f34/fcto_myrdd_fuel_cells.pdf

[40] Pedeferri, P. (2018) Corrosion Science and Engineering. 1st Edition, Springer, Cham.
https://doi.org/10.1007/978-3-319-97625-9